Liquid Crystals
Publication details, including instructions for authors and subscription information:
http://www.informaworld.com/smpp/title~content=t713926090

The synthesis and mesomorphic behaviour of tetracatenar and hexacatenar bi-1,3,4-oxadiazole derivatives

Peng Zhang[a]; Binglian Bai[a]; Haitao Wang[a]; Songnan Qu[a]; Zhixin Yu[a]; Xia Ran[a]; Min Li[a]
[a] Key Laboratory of Automobile Materials, Ministry of Education, Institute of Materials Science and Engineering, Jilin University, Changchun 130012, People's Republic of China

To cite this Article Zhang, Peng , Bai, Binglian , Wang, Haitao , Qu, Songnan , Yu, Zhixin , Ran, Xia and Li, Min(2009) 'The synthesis and mesomorphic behaviour of tetracatenar and hexacatenar bi-1,3,4-oxadiazole derivatives', Liquid Crystals, 36: 1, 7 — 12
To link to this Article: DOI: 10.1080/02678290802638407
URL: http://dx.doi.org/10.1080/02678290802638407

Liquid Crystals,
Vol. 36, No. 1, January 2009, 7–12

The synthesis and mesomorphic behaviour of tetracatenar and hexacatenar bi-1,3,4-oxadiazole derivatives

Peng Zhang, Binglian Bai, Haitao Wang, Songnan Qu, Zhixin Yu, Xia Ran and Min Li*

Key Laboratory of Automobile Materials, Ministry of Education, Institute of Materials Science and Engineering, Jilin University, Changchun 130012, People's Republic of China

(Received 1 September 2008; final form 20 November 2008)

Symmetrical four-chained (tetracatenar) and six-chained (hexacatenar) bi-1,3,4-oxadiazole ester derivatives, namely 5,5′-bis[phenyl(3,4-dialkoxybenzoate)]-2,2′-bi-1,3,4-oxadiazole (C*n*, *n*=6, 10, 12, 14, 16) and 5,5′-bis[phenyl(3,4,5-trialkoxybenzoate)]-2,2′-bi-1,3,4-oxadiazole (D*n*, *n*=7, 10, 14, 16) were synthesised. The liquid crystalline properties were investigated by differential scanning calorimetry, polarised optical microscopy and wide angle X-ray diffraction. It was revealed that the hexacatenar derivatives (D*n*) are non-mesomorphic, while the tetracatenar ones (C*n*) showed a classic progression from smectic C phases (for C6 and C10) to a hexagonal columnar (Col_h) phase (for C12, C14 and C16) with the increase in length of the terminal chains. Molecules of C*n* (*n*=6, 10) tilt about 55-56° from the layer normal within their SmC phase.

Keywords: bi-1,3,4-oxadiazole derivatives; high-angle tilting; biforked mesogens; hexagonal columnar phase

1. Introduction

In recent years, interest in mesomorphic heterocyclic compounds has dramatically increased due to their diversified molecular architectures and distinct mesomorphic properties (*1, 2*). 1,3,4-Oxadiazole derivatives, a type of five-membered heterocyclic compound consisting of nitrogen and oxygen atoms, are one of the most widely investigated classes (*2–6*). In connection with the considerable theoretical and technological interest in bent-core achiral molecules (*7*), substituted 1,3,4-oxadiazole derivatives become more significant. The introduction of five-membered heterocycles into the central core of calamitic molecules results in some novel mesophases due to the dipolar moment and the bent angle (*8–15*). For example, Watanabe et al. reported that 1,3,4-oxadiazole-based molecules exhibit an interesting polymorphism which includes not only the well-known calamitic mesophases (*8*), i.e. nematic, smectic A and smectic C phases, but also B*x* phase in the lower temperature region. Such a polymorphism, including both banana and calamitic liquid crystalline phases, is attributed to the moderate bend angle of the oxadiazole cores.

Recently, we reported the synthesis and mesomorphic behaviour of several bi-1,3,4-oxadiazole derivatives (Scheme 1) (*16–18*). For example, rod-like molecules (BBOXD-*n*) containing bi-1,3,4-oxadiazole rings as a part of the rigid core exhibited SmC phase, within which molecules showed a large-angle tilting (θ>55°) from the layer normal (*16*). Electron donor–acceptor (DA) interaction was considered to be responsible for the large-angle tilting and relatively large transitional enthalpic values.

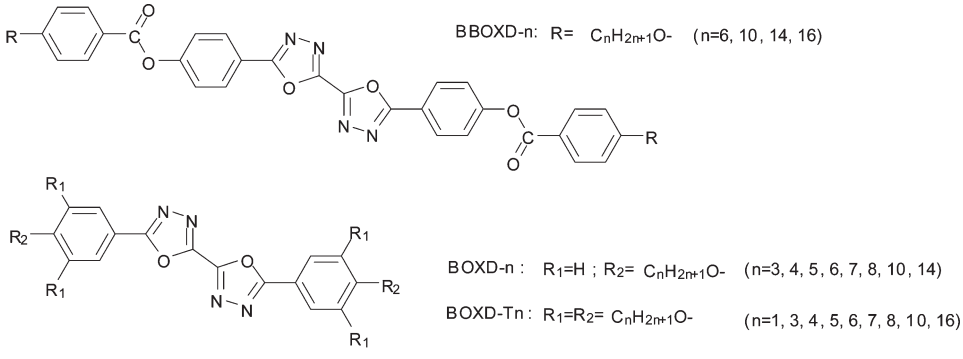

Scheme 1. The molecular structures of BBOXD-*n*, BOXD-*n* and BOXD-T*n*.

*Corresponding author. Email: minli@mail.jlu.edu.cn

ISSN 0267-8292 print/ISSN 1366-5855 online

DOI: 10.1080/02678290802638407
http://www.informaworld.com

Meanwhile, BOXD-*n* regarded as DAAD molecules were designed through rational incorporation of bi-1,3,4-oxadiazole between two coplanar phenyl rings (*17*). The results of X-ray single-crystal analysis, scanning tunnelling microscopy and computer simulation confirmed the presence of both strong face-to-face and edge-to-edge DA interactions in BOXD-*n*. Furthermore, we reported the synthesis and mesomorphic properties of twin-tapered bi-1,3,4-oxadiazole derivatives BOXD-T*n* (n=3, 4, 5, 6, 7, 8, 10, 14), which give rise to columnar mesophases and exhibit strong blue fluorescent emission either in cyclohexane or in bulk (*18*).

In this work, as part of our continuing effort in oxadiazole derivatives, we report the synthesis and liquid crystalline behaviour of symmetrical four-chained (tetracatenar) and six-chained (hexacatenar) bi-1,3,4-oxadiazole ester derivatives, namely 5,5′-bis[phenyl (3,4-dialkoxybenzoate)]-2,2′-bi-1,3,4-oxadiazole (C*n*, n=6, 10, 12, 14, 16) and 5,5′-bis[phenyl (3,4,5-trialkoxybenzoate)]-2,2′-bi-1,3,4-oxadiazole (D*n*, n=7, 10, 14, 16). The tetracatenar derivatives showed a classic progression from smectic C phase (for C6 and C10) to a hexagonal columnar (Col_h) phase for (C12, C14 and C16) with the increase of terminal chain length, while the hexacatenar derivatives are non-mesomorphic.

2. Experimental

2.1. Characterisation

^{1}H NMR spectra were recorded with a Mercury-300BB 300 MHz spectrometer, using $CDCl_3$ as a solvent and tetramethylsilane (TMS) as an internal standard (δ=0.00 ppm). ^{13}C NMR spectra were recorded with a Varian-300 EX spectrometer, using $CDCl_3$ as a solvent and $CDCl_3$ as an internal standard (δ=77.00 ppm). Phase transitional properties were investigated with a Netzsch DSC 204. The rate of heating and cooling was 10°Cmin^{-1}; the weight of the sample was about 3 mg, and indium and zinc were used for calibration. The peak maximum was taken as the phase transition temperature. Texture observation was conducted on a Leica DMLP polarising optical microscope equipped with a Leitz 350 microscope heating stage. X-ray diffraction was carried out with a Bruker Avance D8 X-ray diffractometer. FTIR spectra were recorded with a Perkin-Elmer spectrometer (Spectrum One B) and the sample was in the form of a pressed tablet with KBr.

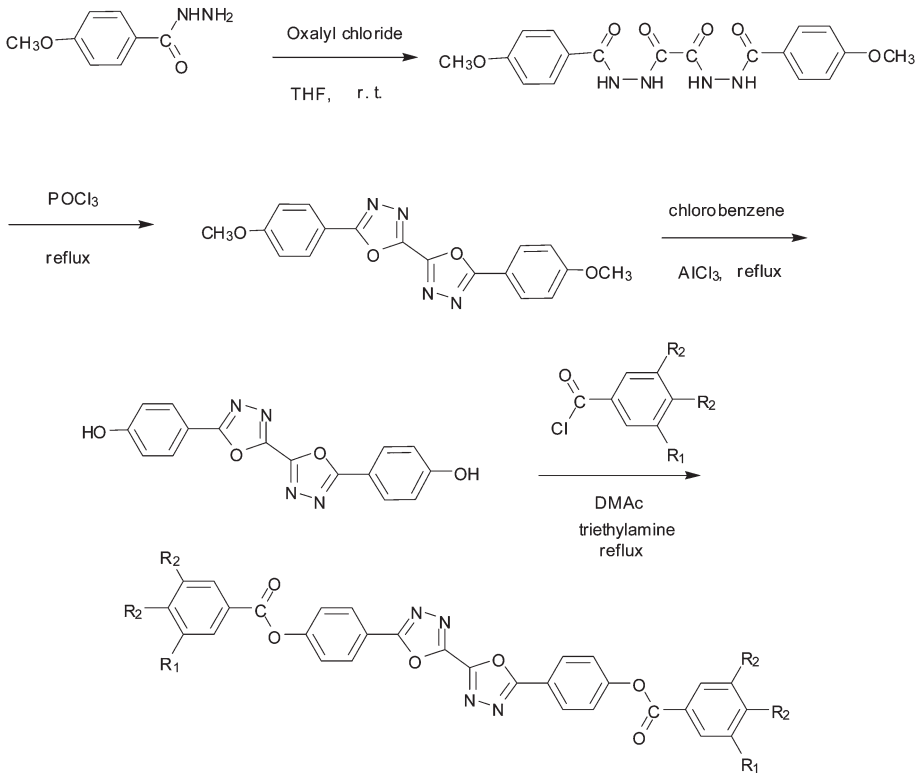

Scheme 2. Synthetic route for C*n* and D*n* compounds.

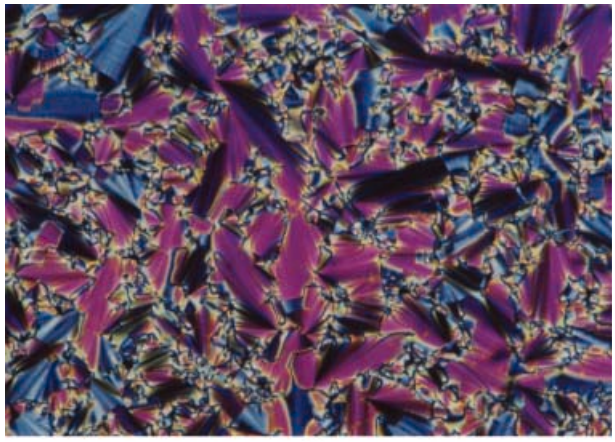

(a)

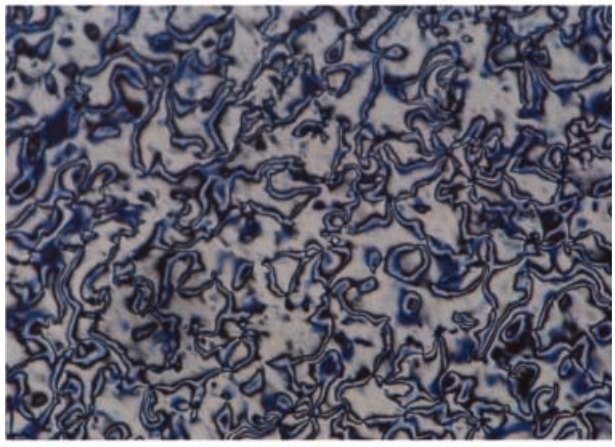

(b)

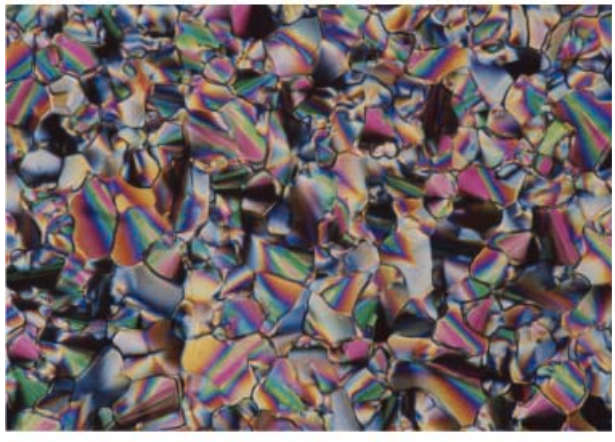

(c)

Figure 1. Polarising optical photomicrographs of C*n* (a) fan-shaped texture of C10 showing SmC phase at 162°C; (b) Schlieren texture of C10 after shearing at 162°C; (c) Pseudo focal conic fan-shaped texture of C16 at 153°C.

2.2 Synthesis

Scheme 2 shows the synthetic route for C*n* and D*n*. The synthesis of C*n* and D*n* is similar to that of mono-substituted analogues, namely 5,5′-bis(phenyl

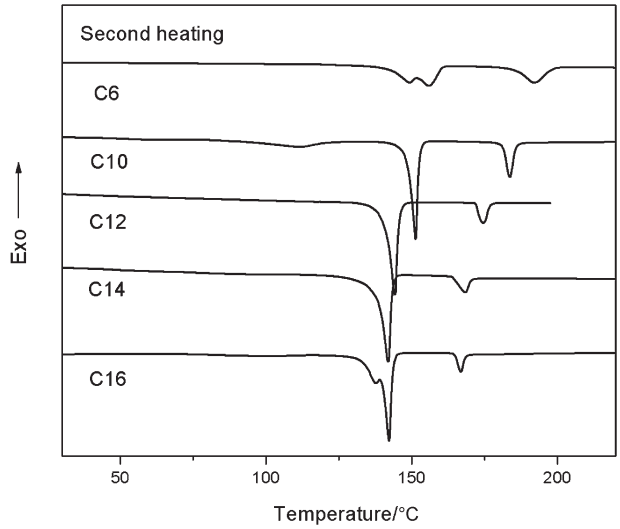

Figure 2. Differential scanning calorimetry curves of C*n* in the second heating runs.

4-alkoxybenzoate)-2,2′-bi-1,3,4-oxadiazole, and a detailed description of the synthesis and purification of the intermediate compounds can be found in our previous work (*16*). The crude products were further purified through a column of silica gel using 2% ethyl acetate in chloroform as eluent to afford C*n* and D*n* for further ^{1}H NMR, ^{13}C NMR, FT-IR measurements and elemental analysis. Yield>63%.

5,5′-bis[4-(3,4-didecyloxybenzoate)phenyl]-2,2′-bi-1,3,4-oxadiazole (C10).

^{1}H NMR (300 MHz, $CDCl_3$), (ppm, from TMS): 8.32 (d, 4H, J=8.7 Hz); 7.84 (dd, 2H, J=1.8 Hz, J=8.7 Hz); 7.67 (s, 2H); 7.46 (d, 4H, J=8.7 Hz); 6.95 (d, 2H, J=8.7 Hz); 4.09 (m, 8H); 1.87 (m, 8H); 1.53 (s, 56H); 0.89 (m, 12H).

^{13}C NMR (300 MHz, $CDCl_3$): δ=165.8, 164.4, 154.8, 154.2, 152.9, 148.7, 129.1, 124.6, 123.0, 120.7, 119.8, 114.6, 111.9, 69.4, 69.1, 31.9, 29.5, 29.4, 29.1, 29.0, 26.0, 25.9, 22.7, 14.1.

FT-IR (KBr, pellet, cm^{-1}): 2954, 2922, 2871, 2850, 1717, 1600, 1549, 1519, 1492, 1470, 1430, 1393, 1346, 1296, 1276, 1201, 1170, 1157, 1138, 1018, 952, 875, 753, 667, 525.

Elemental analysis: calculated for $C_{70}H_{98}N_4O_{10}$ (%), C, 72.76; H, 8.55; N, 4.85; Found, C, 72.89; H, 8.44; N, 4.57.

5,5′-bis[4-(3,4,5-tridecyloxybenzoate)phenyl]-2,2′-bi-1,3,4-oxadiazole (D10).

^{1}H NMR (300 MHz, $CDCl_3$), (ppm, from TMS): 8.33 (d, 4H, J=9.0 Hz); 7.45 (d, 4H, J=8.7 Hz); 7.42 (s, 4H); 4.06 (m, 12H); 1.85 (m, 12H); 1.50 (m, 12H); 1.28 (s, 72H); 0.88 (m, 18H).

Table 1. Transition temperatures (°C) and transition enthalpies (kJ/mol, in parentheses) for the C*n* series[a].

Comp.	*First cooling*	*Second heating*
C6	I 189 (14.8) SmC 142 (23.8) Cr	Cr 149 (18.9) Cr 156 (13.6) SmC 192 (14.8) I
C10	I 181 (12.2) SmC 140 (29.4) Cr 119(11.9) Cr	Cr 111 (14.5) Cr 151 (35.5) SmC 183(13.0) I
C12	I 171(11.1) Col_h 138(52.4) Cr	Cr 144(53.2) Col_h 174(11.3) I
C14	I 166 (9.7) Col_h 137 (60.2) Cr	Cr 141 (59.8) Col_h 168(10.0) I
C16	I 165 (8.8) Col_h 137 (52.3) Cr 117(38.4) Cr	Cr 138(29.5) Cr 142 (44.0) Col_h 167(7.7) I

[a]Col_h, SmC, Cr and I indicate hexagonal columnar phase, smectic C phase, crystalline phase and isotropic liquid, respectively.

^{13}C NMR (300 MHz, $CDCl_3$): δ=165.8, 164.4, 154.7, 153.0, 152.9, 143.4, 129.2, 123.1, 120.0, 108.7, 73.6, 69.3, 31.9, 30.3, 29.7, 29.6, 29.4, 29.3, 26.1, 22.7, 14.1.

FT-IR (KBr, pellet, cm^{-1}): 2923, 2853, 1743, 1610, 1593, 1554, 1491, 1469, 1433, 1418, 1385, 1338, 1233, 1218, 1198, 1163, 1130, 1120, 1077, 1015, 992, 953, 936, 867, 746, 730, 698, 522.

Elemental analysis: calculated for $C_{90}H_{138}N_4O_{12}$ (%), C, 73.63; H, 9.47; N, 3.82; Found, C, 73.61; H, 9.47; N, 3.68.

Melting points: 137°C for D7, 108°C for D10, 98°C for D14 and 94°C for D14.

3. Results and discussion

The phase behaviour of C*n* and D*n* was studied by polarising optical microscopy, differential scanning calorimetry (DSC), and wide-angle X-ray diffraction. The compounds D*n* (*n*=7, 10, 14, 16) are non-mesomorphic. They exhibited a spherically crystal texture on cooling from the isotropic liquid. During cooling from the isotropic melt of C10, the growth of elongated germs, so-called smectic batonnets, are observed from the black background (*19*). The compound C10 showed a fan-shaped texture (Figure 1(a)) and gave a lined schlieren texture on shearing (Figure 1(b)) at 162°C Furthermore, schlieren coexistence a with fan-shaped texture was observed in cooling runs, indicating the existence of SmC phase. Pseudo focal conic fan-shaped texture (Figure 1(c)), typical for a columnar phase, was observed for the C*n* (*n*=12, 14, 16) with long terminal alkyl chains.

The DSC curves of the C*n* are given in Figure 2. The transition temperatures and the associated enthalpy changes of the compounds C*n* are summarised in Table 1. It can be seen that the lower homologues of C*n* (*n*=6, 10) exhibited enantiotropic SmC phase, while the higher ones C*n* (*n*=12, 14, 16) exhibited enantiotropic columnar phase.

In order to reveal the molecular packing in their mesophases, variable temperature X-ray diffraction (XRD) experiments were performed on C*n*. A characteristic XRD pattern of smectic phase was observed for C6 (as shown in Figure 3(a)), which contains two sharp peaks (d_{100}=24.3 Å, d_{200}=12.1 Å) in a low-angle region, implying the formation of a layered structure, and a broad halo in the wide-angle region centred at a spacing of 4.6 Å, indicating a liquid-like arrangement of the molecules within the layers. Considering that the layer spacing of C6 (24.3 Å at 160°C) is much shorter than its molecular length in the fully extended configuration (42.9 Å), C6 exhibited SmC phase. A similar mesomorphic structure was observed in C10 during cooling from the isotropic state. Data for layer spacings (*d*), molecular lengths (*l*), and *d*/*l* ratios of C*n* in their mesophases were collected in Table 2. The layer

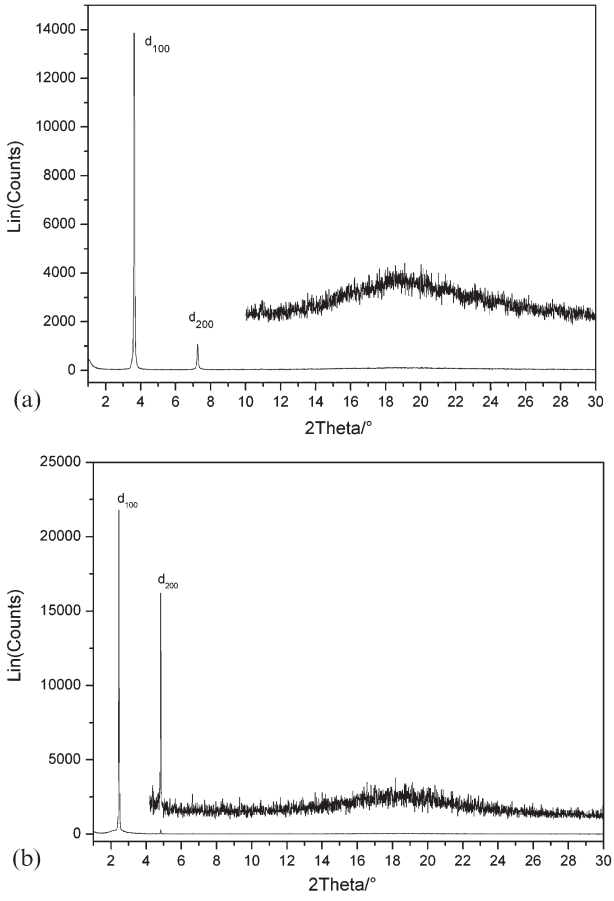

Figure 3. X-ray diffraction patterns of (a) C6 at 160°C and (b) 16 at 152°C.

Table 2. WAXD results for C*n* in their liquid crystalline phases.

Compound	[a]Molecular length(ℓ) (Å)	Mesophase	d_{obsd} (Å)	d/ℓ	Θ(°)	Lattice parameter (Å)
C6	42.9	SmC (160°C)	24.3, 12.1	0.57	55.6	
C10	52.6	SmC (170°C)	29.4, 15.2	0.56	56.1	
C12	57.5	Col_h (155°C)	33.3, 16.8			a=38.5.
C14	62.2	Col_h (150°C)	34.4, 17.5			a=39.7
C16	66.9	Col_h (152°C)	36.0, 18.3			a=41.6

[a]Molecular length was calculated by MM2.

spacings (d) were measured to be much smaller than the estimated all-trans molecular lengths of the most extended conformation, and the d/l ratios were in the range of 0.5 to 0.6. Thus, the molecules of C*n* (n=6, 10) exhibited large tilting (ca. 55.6 to 56.1°) from the layer normal within their smectic C phases.

The XRD patterns of C16 in the mesophase (Figure 3(b)) consisted of one strong (d=36.0 Å) peak and one weak (d=18.3 Å) peak in the small-angle regions as well as a diffuse halo centred at 4.6 Å. A similar XRD pattern was observed for compounds C12 and C14 in their mesophases. To indentify the type of mesophase, miscibility experiments were carried out between C6 and the higher ones C*n* (n=14, 16). We found that the mesophase of either C14 or C16 is immiscible with that of C6. Therefore, the mesophase is thought to be a columnar phase which is different from the classic smectic C phase. So, the mesophase of C12, C14 and C16 was identified as Col_h although the reflection characterising the hexagonal columnar structure (*11*) was not observed in the present case. The peak in the small-angle region was assigned to reflection (*10*), thus the two dimensional hexagonal arrangement of the columns with a lattice parameter of a=41.6 Å. The estimated all-trans molecular length of the most extended conformation of C16 is 66.9 Å, obtained by the MM2 method. The number of molecules within one disk was calculated to be three (*20, 21*) assuming that the density of C16 in the mesophase is 1 g cm^{-3}.

In summary, tetra- and hexacatenar bi-1,3,4-oxadiazole derivatives were synthesised and the tetracatenar derivatives C*n* were demonstrated to exhibit either smectic C or Col_h phase depending on the length of terminal alkyl chains. Molecules of short-chain derivatives of C*n* (n=6, 10) exhibited high-angle tilting within their smectic C phases, which is similar to that of dicatenar bi-1,3,4-oxadiazole derivatives (BBOXD-*n*, BOXD-*n*) reported in our previous work (*16, 17*). Considering the structural similarity of their rigid core, intermolecular DA interaction was expected in the present C*n* series. Increasing the length of the terminal chains causes the appearance of hexagonal columnar phase of C*n* (n=12, 14, 16). The transition from SmC to hexagonal columnar phase of C*n* with the increase of length of terminal chains is attributed to the strong curvature of the core–chain interface in this phasmidic columnar phase (*22*).

Acknowledgements

The authors are grateful to the National Science Foundation Committee of China (project No. 50373016), Program for New Century Excellent Talents in Universities of China Ministry of Education, Special Foundation for PhD Program in Universities of China Ministry of Education (Project No. 20050183057) and Project 985-Automotive Engineering of Jilin University for their financial support of this work.

References

(1) Dingemans T.J.; Murthy N.S.; Samulski E.T. *J. Phys. Chem. B* **2001**, *105*, 8845–8860.
(2) Schulz B.; Orgzall I.; Freydank A.; Xu C.G. *Adv. Colloid Interface Sci.* **2005**, *116*, 143–164.
(3) Kim B.G.; Kim S.; Park S.Y. *Tetrahedron Lett.* **2001**, *42*, 2697–2699.
(4) Zhang Y.D.; Jespersen K.G.; Kempe M.; Kornfield J.A.; Barlow S.; Kippelen B.; Marder S.R. *Langmuir* **2003**, *19*, 6534–6536.
(5) Lai C.K.; Ke Y.C.; Su J.C.; Lu C.S.; Li W.R. *Liq. Cryst.* **2002**, *29*, 915–920.
(6) Wen C.R.; Wang Y.J.; Wang H.C.; Sheu H.S.; Lee G.H.; Lai C.K. *Chem. Mater.* **2005**, *17*, 1646–1654.
(7) Niori T.; Sekine T.; Watanabe J.; Furukawa T.; Takezoe H. *J. Mater. Chem.* **1996**, *6*, 1231–1233.
(8) Kang S.; Saito Y.; Watanabe N.; Tokita M.; Takanishi Y.; Takezoe H.; Watanabe J. *J. Phys. Chem. B* **2006**, *110*, 5205–5214.
(9) Dingemans T.J.; Samulski E.T. *Liq. Cryst.* **2000**, *27*, 131–136.
(10) Madsen L.A.; Dingemans T.J.; Nakata M.; Samulski E.T. *Phys. Rev. Lett.* **2004**, *92*, 145505.
(11) Acharya B.R.; Primak A.; Kumar S. *Phys. Rev. Lett.* **2004**, *92*, 145506.
(12) Gortz V.; Goodby J.W. *Chem. Commun.* **2005**, *26*, 3262–3264.
(13) Semmler K.J.K.; Dingemans T.J.; Samulski E.T. *Liq. Cryst.* **1998**, *24*, 799–803.
(14) Reddy R.A.; Tschierske C. *J. Mater. Chem.* **2006**, *16*, 907–961.
(15) Choi S.; Kang S.; Takanishi Y.; Ishikawa K.; Watanabe J.; Takezoe H. *Chirality* **2007**, *19*, 250–254.

(16) Zhang P.; Qu S.; Wang H.; Bai B.; Li M. *Liq. Cryst.* **2008**, *35*, 389–394.
(17) Qu S.; Chen X.; Shao X.; Li F.; Zhang H.; Wang H.; Zhang P.; Yu Z.; Wu K.; Wang Y.; Li M. *J. Mater. Chem.* **2008**, *18*, 3954–3964.
(18) Qu S.; Li M. *Tetrahedron* **2007**, *63*, 12429–12436.
(19) Dierking I. *Textures of Liquid Crystals*; Wiley-VCH: Weinheim, 2003, p. 91.
(20) Borisch K.; Diele S.; Goring P.; Kresse H.; Tschierske C. *J. Mater. Chem.* **1998**, *8*, 529–543.
(21) George M.; Weiss R.G. *Langmuir* **2002**, *18*, 7124–7135.
(22) Nguyen H.T.; Destrade C.; Malthete J., In *Handbook of Liquid Crystals*; Demus D., Goodby J., Gray G.W., Spiess H.W., Vill V. (Eds), Wiley-VCH: Weinheim, 1998; Vol. 2B Chapter 7.